Journal of Chromatography A, 1364 (2014) 12–19

Contents lists available at ScienceDirect

Journal of Chromatography A

journal homepage: www.elsevier.com/locate/chroma

Design of a surface-immobilized 4-nitrophenol molecularly imprinted polymer via pre-grafting amino functional materials on magnetic nanoparticles

Ali Mehdinia [a,*], Sahar Dadkhah [b], Tohid Baradaran Kayyal [b], Ali Jabbari [b]

[a] Department of Marine Science, Iranian National Institute for Oceanography and Atmospheric Science, Tehran, Iran
[b] Department of Chemistry, Faculty of Science, K. N. Toosi University of Technology, Tehran, Iran

ARTICLE INFO

Article history:
Received 24 June 2014
Received in revised form 12 August 2014
Accepted 18 August 2014
Available online 23 August 2014

Keywords:
Surface imprinted polymer
Immobilized template
Pre-grafted functional material
Magnetic nanoparticles
4-Nitrophenol

ABSTRACT

In order to resolve the low adsorption capacity of the surface molecularly imprinting methods, an approach was developed for the preparation of magnetic imprinted polymers by pre-grafting the amino functional material, 3-aminopropyltriethoxysilane (APTES), on the surface of the silica coated magnetic substrate. APTES was used for amino functionalization of the silica coated Fe_3O_4 nanoparticles. Amino groups were used for immobilization of the template molecules on the magnetic surface and additionally to react with the terminal vinyl groups of cross-linker, ethylene glycol dimethacrylate (EGDMA), by the Michael addition reaction. In this way, the imprinting sites of the analytes formed on the substrate were increased. The sorbent was synthesized in the presence of 4-nitrophenol (4-NP) and EGDMA as the template and cross-linker, respectively. Different parameters affecting the adsorption, such as pH, desorption solvent type and adsorption time were evaluated and optimized. The prepared magnetic molecularly imprinted polymer (MMIP) showed high adsorption capacity and proper selectivity for the template molecule. The kinetic adsorption curve indicated that 90 min was sufficient to achieve the adsorption equilibrium for MMIP. The maximum adsorption capacity was 129.1 mg g^{-1}. The experiments exhibited a linear range of 10–3000 μg L^{-1} for 4-NP with the correlation coefficient (R^2) of 0.997. The results of the real sample analysis confirmed the applicability of the proposed MMIP for quantitative analysis of 4-NP in the aqueous samples.

1. Introduction

Molecularly imprinted polymers (MIPs) are common, robust and cost-efficient smart materials which are used to prepare a qualified substrate with selective recognition properties for the target molecules. The selective recognition sites are created by a process where the template molecules are imprinted into the polymeric matrices. During the recent decades, great attention was focused on improving synthesis conditions of MIPs. Surface imprinting is now among the most studied alternative methods to overcome the drawbacks related to the traditional MIPs such as bulk polymerization [1–3]. Surface graft imprinting improves the adsorption capacity, kinetic of binding and mass transfer in MIPs by controlling the position of the templates on the material's surfaces or in their vicinity. Several strategies have been proposed for the surface imprinting, such as the use of immobilized initiators on the supporting matrix [4], atom transfer radical polymerization (ATRP) [5,6], reversible addition fragmentation chain transfer (RAFT) polymerization [7] and grafting polymerization by modifying the surface [8].

Nanoparticles are promising support materials for the surface imprinting that expresses notable advantages owing to their large external surface area to volume ratio. Furthermore, the utilization of nanoparticles leads to enhancement of the physical and chemical properties of the sorbent, such as uniform spherical geometry, as well as stability and facile dispersion [9]. The perfect size of MIP nanoparticles can be achieved by the selection of proper nanostructured substrates and the control of imprinted layer thicknesses [3]. Different substrates were used as a support in the surface imprinting process, such as activated silica nanoparticles [2,10,11], Fe_3O_4 nanoparticles [12,13], gold nanoparticles [14], titanium dioxide [15], chitosan [16], activated polystyrene beads [4], quantum dots [17,18], alumina membranes [19], carbon nanotubes [20,21] and graphene [22].

* Corresponding author. Tel.: +98 21 66944873; fax: +98 66944869.
E-mail addresses: mehdinia@inio.ac.ir, mehdi_3848@yahoo.com (A. Mehdinia).

http://dx.doi.org/10.1016/j.chroma.2014.08.058
0021-9673/

Recently, the frequently studied method for selective extraction of templates is based on the combination of magnetic nanoparticles and imprinting polymers. The encapsulation of magnetic components into the MIPs can create a selective composite polymer with magnetically susceptible characteristics [23].

In order to prepare the imprinted polymers, the functional groups undertake critical roles via binding to the target molecules before the actual imprinting [24]. An efficient procedure for creating the imprinted sites is based on an interaction between the pre-grafted functional material and template molecules rather than that between the template and functional monomers in the bulk solution. The pre-grafting of functional groups on the surface can also increase the imprinting sites formed for the target analytes. In the present technique, the templates were at first immobilized on the functionalized substrate through an effective non-covalent interaction [25–28]. Thereafter, the post-imprinting of the template molecules occurs in the grafted groups toward the reactive end groups of the special cross-linking agent. Therefore, the method demonstrates an effective approach to the surface imprinting methodology via immobilizing the template on the support material.

Nitrophenols are classified as priority and persistent contaminants due to their relatively high toxicity, even at trace level concentrations in the aqueous matrices [27]. Since these compounds are released into the aquatic environments through the effluents of various industries, the U.S. Environmental Protection Agency (U.S. EPA) has listed them as toxic pollutants. Among the mono nitrophenols, 4-nitrophenol (4-NP) is often considered owing to its high production in the world, toxicity and water solubility [28]. Because of the low concentration and high water solubility of 4-NP, and also the presence of much interferences in the water samples, the clean-up and pre-concentration steps are required. In this regard, different MIPs were developed for the selective and sensitive recognition of 4-NP [28–32].

In our previous work [31], we synthesized magnetic imprinted polymer via the "Grafting to" techniques for the selective recognition of 4-NP in the aqueous samples. The magnetic surface was at first modified via vinyl groups and then employed for the grafting polymerization of the functional monomer and cross-linker in the presence of target analytes. In the present work, an effective approach was developed for the preparation of magnetic MIP (MMIP) via pre-grafting of functional groups on the magnetic nanoparticles surface. Therefore, 4-NP was also used to evaluate the performance of the template immobilizing approach which are used here, than that the "Grafting to" method, used in our previous work. Template immobilizing was performed using 3-aminopropyltriethoxysilane (APTES) to associate the target analyte on the surface of the magnetic substrate. The post imprinting was also successfully performed by ethylene glycol dimethacrylate (EGDMA) in the presence of 2,2-azobisisobutyronitrile (AIBN). The results showed that the static adsorption capacity of the MMIP, prepared by the pre-grafting approach, was about two-folds as compared to that obtained in our previous work. It clearly confirmed the improvement of the adsorption capacity, number of sites and binding kinetic of the prepared MMIP.

2. Experimental

2.1. Materials

4-Nitrophenol (4-NP), 2-nitrophenol (2-NP), 2,4-dinitrophenol (2,4-DNP), phenol (Ph), 3-aminopropyltriethoxysilane (APTES) and 2,2-azobisisobutyronitrile (AIBN) were obtained from Merck (Darmstadt, Germany). Ethylene glycol dimethacrylate (EGDMA) and acetonitrile (HPLC grade) were purchased from Sigma–Aldrich (Beijing, China) and Caledon (Ontario, Canada) companies, respectively. Toluene, methanol (HPLC grade), iron (III) chloride hexahydrate ($FeCl_3{\cdot}6H_2O$), iron (II) chloride tetrahydrate ($FeCl_2{\cdot}4H_2O$), ammonium hydroxide and tetraethyl orthosilicate (TEOS) were also obtained from Merck (Darmstadt, Germany).

2.2. Instruments

The size, structure and morphology of the MMIPs were characterized by transmission electronic microscopy (Zeiss – EM10C – 80 kV TEM) and scanning electron microscopy (SEM Vega tescan), respectively. A Fourier transform infrared FT-IR (Bruker VERTEX 70 spectrometer) was utilized to investigate the infrared spectra of MMIPs using KBr pellets.

2.3. HPLC analysis

All chromatographic measurements were performed, using an Agilent 1100 high performance liquid chromatograph (Santa Clara, CA, USA) with a C_{18} column (250 mm × 4.6 mm i.d., 5 μm) and UV/vis detector. For quantitative analysis of 4-NP, a RP-HPLC method was used. The mobile phase for chromatographic analysis consisted of acetonitrile, containing 1% (v/v) acetic acid, as solvent A and Milli-Q water acidified to pH 2.5 with acetic acid, as solvent B. The gradient profile was 50–100% A from 0 to 10 min, and then isocratic elution for 2 min at a flow rate of 1 mL min^{-1}. All compounds were detected at 254 nm and the oven temperature was set at 25 °C.

2.4. Preparation of silica-based magnetic nanoparticles

The preparation of Fe_3O_4 nanoparticles was carried out by mixing $FeCl_3{\cdot}6H_2O$ (34.6 mmol) and $FeCl_2{\cdot}4H_2O$ (17.30 mmol) with 160 mL double distilled water, while being stirred under nitrogen gas atmosphere. Then, 20 mL of ammonium hydroxide (25%, v/v) was added drop wise to the solution while elevating the temperature of the solution up to 80 °C. The reaction was kept at the mentioned temperature for 30 min. The obtained Fe_3O_4 nanoparticles were dispersed in the mixture of ethanol (160 mL) and water (40 mL) by sonication for 15 min, then ammonium hydroxide (15 mL) and TEOS (2.1 mL) were added to the reaction mixture. The reaction was carried out for 12 h at 40 °C under continuous mechanical stirring. The final product was isolated by an external magnetic field, and then, thoroughly washed with ethanol and water, respectively.

2.5. Surface modification and pre-grafting functional material

Fe_3O_4@SiO_2 (400 mg), APTES (1 mL) and absolutely dry toluene (30 mL) were mixed in a flask under nitrogen atmosphere. The reaction was refluxed for 48 h under continuous mechanical stirring. The resulted pre-grafted amino-functionalized nanoparticles were washed with toluene and methanol thoroughly, and then dried at 55 °C for 3 h.

2.6. Preparation of the surface-immobilized 4-NP-MMIP

The template adsorption on the amino-functional nanoparticles was carried out in 20 mL acetonitrile, 0.4 mmol 4-NP and 200 mg modified magnetic silica at 0–2 °C for 12 h to obtain the modified magnetic silica self-assembled by 4-NP. Then, the cross-linker (EGDMA, 4 mmol) was added. The mixture was stirred for 30 min for the preparation of the preassembled solution. After sealing, shaking and purging the mixture with nitrogen, a 20 mL of acetonitrile solution containing 40 mg of AIBN was added to the reaction mixture while it was being sonicated and purged by the nitrogen gas in an ice bath for 15 min. The polymerization was performed

by exposing the mixture to 60 °C in an oil bath for 24 h, under nitrogen atmosphere. The synthesized product was separated and washed with methanol/acetic acid (9:1, v/v) several times until the template molecules were not detected in the washing solution. Magnetic non-imprinted polymers (MNIPs) were synthesized using the same synthetic protocol mentioned above without the template addition.

2.7. Evaluation of static adsorption capacity and selectivity

The adsorption capacity of the sorbent was measured three times by suspending 20 mg of 4-NP-MMIPs or MNIPs in a 10 mL aqueous solution of 4-NP with various concentrations ranging from 0.1 to 9 mM. The mixture was shaken for 12 h at room temperature and then, the magnetic sorbent was separated using a magnet. The supernatant solution was analyzed by RP-HPLC. The adsorption capacity (Q) was calculated based on the Eq. (1):

$$Q = \frac{(C_0 - C_e)V}{m} \quad (1)$$

where Q (mg g^{-1}) is the adsorption capacity, and C_0 and C_e (mg L^{-1}) are the initial and equilibrium concentrations of 4-NP solution, respectively. V (L) is volume of the initial solution and m (g) is the weight of the adsorbent (MMIP).

The selectivity of the prepared MMIP is evaluated via several structural analogs of 4-NP. In this regard, 2-NP, 2,4-DNP, Ph were chosen. They contained similar functional groups with the analyte and were used to examine the recognition selectivity of the synthetic MMIPs toward 4-NP. The selectivity recognition experiments of each compound were carried out by adding 20 mg MMIPs (or MNIPs) into 10 mL solution of each phenolic compound with the concentration level of 500 mg L^{-1}. The distribution coefficient was calculated according to Eq. (2).

$$k_d = \frac{Q_e}{C_e} \quad (2)$$

where k_d represents the distribution coefficient (L g^{-1}), Q_e (mg g^{-1}) is the equilibrium adsorption capacity and C_e (mg L^{-1}) is the equilibrium concentration. The selectivity coefficient of MMIP can be obtained from the equilibrium binding data according to the Eq. (3):

$$\alpha = \frac{k_{d(\text{template})}}{k_{d(\text{sc})}} \quad (3)$$

where α is the selectivity coefficient and $k_{d(\text{sc})}$ is the distribution coefficient of similar compounds. A relative selectivity coefficient α_r (Eq. (4)) can also indicate the enhanced extent of adsorption affinity and selectivity of MMIP to the templates with respect to MNIP.

$$\alpha_r = \frac{\alpha_{\text{MIP}}}{\alpha_{\text{NIP}}} \quad (4)$$

2.8. Real sample analysis

The seawater of the Persian Gulf was collected and stored in the pre-cleaned glass bottles before conducting the analysis. The sample was filtered to eliminate particulate matters and also it was stored in a dark and cool place. The proposed procedure was applied for the determination of 4-NP in real water sample. 20 mg of magnetic sorbent was added to 10 mL of the water sample, and stirred for 90 min at 25 °C. Subsequently, the MMIP was separated by an external magnetic field and eluted with 0.5 mL of methanol solution containing 10% acetic acid. Finally, the concentration of 4-NP in the eluted solution was determined by HPLC-UV.

3. Results and discussion

3.1. Preparation and characterization of MMIP

The surface-immobilized template imprinting polymer was obtained by the following steps: (I) synthesis of Fe_3O_4 nanoparticles, (II) silica coating on Fe_3O_4, (III) surface functionalization by APTES, (IV) immobilization of the templates on the surface (V) Michael addition reaction between EGDMA and amino groups of APTES and (VI) coating thin layer of MIP on the surface. The schematic representation of the preparation procedure of the sorbent is illustrated in Fig. 1.

The preparation of Fe_3O_4 nanoparticles was carried out by the coprecipitation method. Silica coating on the Fe_3O_4 was carried out by a sol–gel process with TEOS. Silica nanoparticles exhibit high surface areas and intrinsic surface reactivity which allows its modification to be performed by a silanization procedure with different silane coupling agents [33]. The silica shell on the surface of the magnetic nanoparticles prevents the aggregation and oxidation of the magnetic particles. The immobilization of the templates on the surface was designed by hydrogen bonding interactions between templates and functional groups. The immobilized template approach prevented the residual template leakage and increased the imprinting efficiency. This is based on the surface functionalization with C–NH_2 groups which can assemble template and cross-linker, simultaneously. The assembling of cross-linker on the magnetic surface was performed via Michael addition reaction. The Michael addition involves the addition of a nucleophile, also called “Michael donor” to an α,β-unsaturated carbonyl compound as a “Michael acceptor”. In this regard, the nitrogen-donor version of the Michael addition is often referred to as the aza-Michael reaction [8,34]. In the present work, an aza-Michael addition reaction occurred between the terminal vinyl groups of the cross-linker as α,β-unsaturated carbonyl and amino functional groups of APTES as nucleophile. Since, there is always a competition between bulk and surface polymerization, the bulk polymerization effect can be minimized by Michael addition of EGDMA prior to the molecular imprinting process. Subsequently a thin film of MIP was formed by the addition of AIBN, in the presence of APTES as amino functional groups, 4-NP as template and the optimal amount of EGDMA as cross-linker.

3.1.1. FT-IR spectroscopic analysis

FT-IR spectra of Fe_3O_4@SiO_2, Fe_3O_4@SiO_2@NH_2 and Fe_3O_4@MIP were obtained to confirm the synthesis of the expected products. The presence of silanol groups on the surface of Fe_3O_4 is shown in Fig. 2(a). The characteristic peak of Fe–O band appeared at around 580.27 cm^{-1} in the spectrum. The Si–O–Si (symmetric), Si–OH and Si–O–Si (asymmetric) vibration peaks were observed at about 801.1 cm^{-1}, 946.07 and 1098.78 cm^{-1}, respectively. It confirmed the silanization of Fe_3O_4 nanoparticles. As shown in Fig. 2, by comparing the FTIR spectra of Fe_3O_4@SiO_2@NH_2 (b) with Fe_3O_4@SiO_2 (a), it was clearly observed that the N–H bending vibration peak at 1608.33 cm^{-1} and the relatively strong peak in 2800–3000 cm^{-1} which are corresponded to the stretching vibration of C–H bonds of the methyl or methylene groups of APTES. The results indicated that modification on the surface of Fe_3O_4@SiO_2 has been successfully achieved by APTES. As shown in Fig. 2(c), the peak that appeared at 1731.08 cm^{-1} is related to the grafting of carbonyl group of EGDMA on the magnetic surface that confirmed the polymerization process has been successful. In addition, the C=O peak in EGDMA (conjugated esters) appears in the region of 1710–1720 cm^{-1}. The shift of C=O peak from this value to 1731.08 cm^{-1} can indicate the elimination of the conjugation of the carbonyl group by Michael addition reaction and polymerization process.

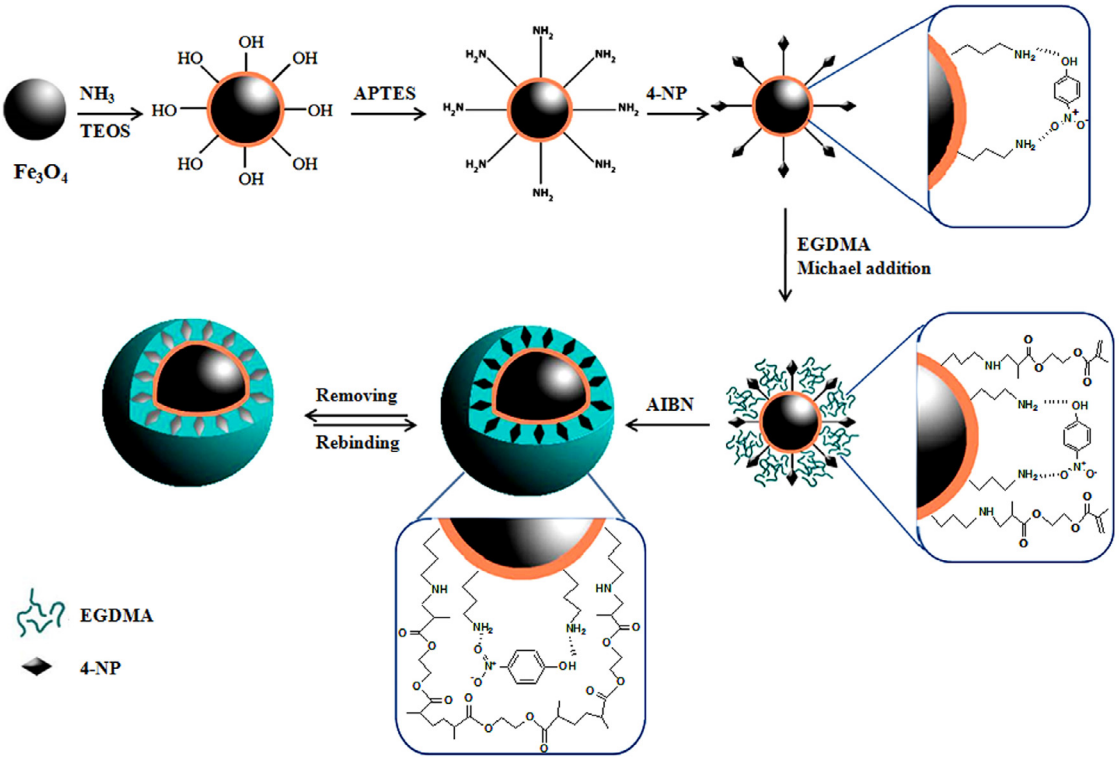

Fig. 1. Scheme of the synthetic route for 4NP-MMIP by surface immobilized template strategy.

3.1.2. SEM and TEM characterizations

The morphology, size and structure of MMIP nanoparticles were assessed by SEM and TEM as shown in Fig. 3. The core–shell structure (polymeric shell) with well specific shape and configuration on the surface of Fe_3O_4@SiO_2 nanoparticles was obviously observed in TEM images. As illustrated in the SEM image, the nanoparticles are spherical with a particle size range and some extent of aggregation. The TEM micrograph also clearly demonstrates the successful synthesis of MIP-coated nanoparticles, and the thickness of imprinted polymer layer was lower than 25 nm.

3.2. Optimization of the extraction parameters

3.2.1. Effect of solution pH

pH plays a special role in controlling the adsorption process due to its effects on the available surface binding sites and ionization of the ionizable analytes such as 4-NP. In this study, the influence of pH was investigated in the range of 2–8. Fig. 4(a) indicates that the MIP provided the highest affinity at pH of 5 for the target analyte. 4-NP was mainly extracted in the molecular form at pH of 5 due to the better H-bonding interaction between the analyte and the

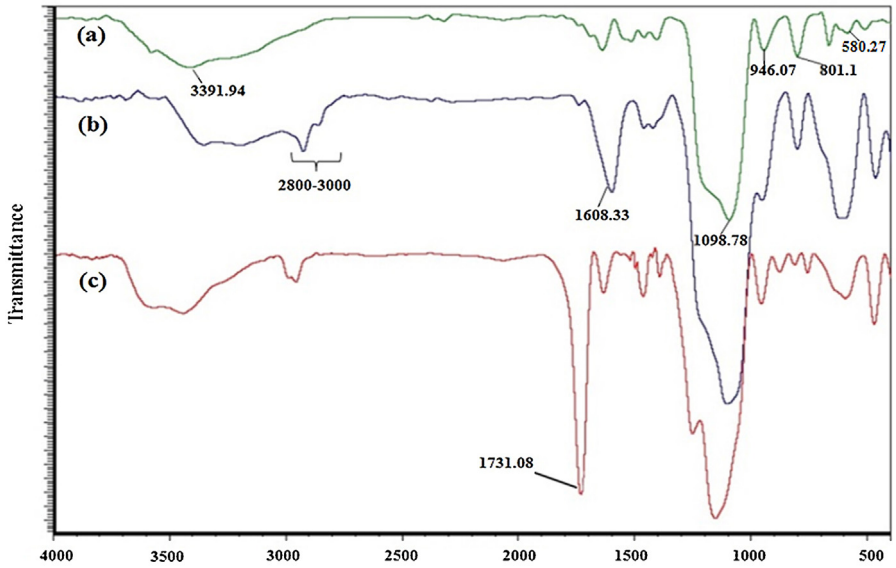

Fig. 2. FT-IR spectra of Fe_3O_4@SiO_2 (a), Fe_3O_4@NH_2 (b) and Fe_3O_4@MIP (c).

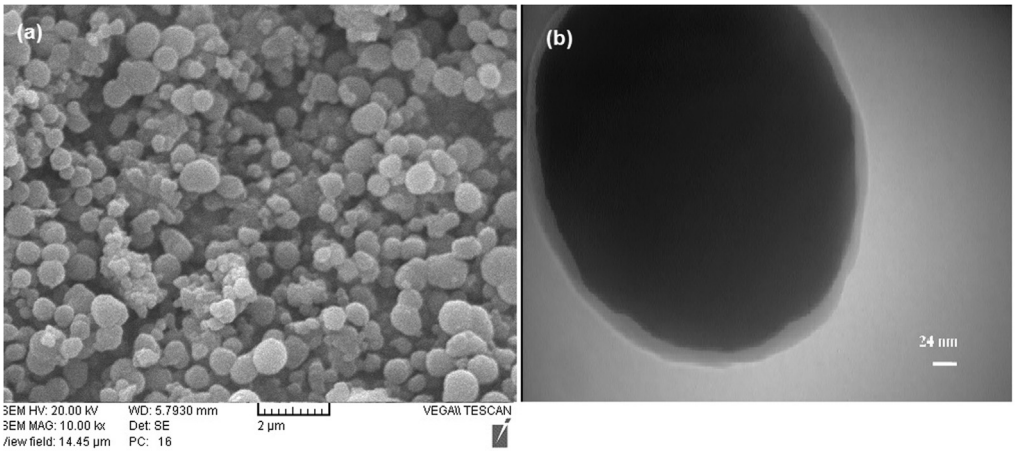

Fig. 3. SEM (a) and TEM (b) images of MMIP.

imprinted binding sites. According to the dissociation constant of 4-NP (pK_a = 7.15), the neutral and acidic form would be the preferred form of it at pH values lower than pK_a.

The cavities of the polymer were imprinted with the neutral form of 4-NP molecule, therefore, when pH increased more than the pK_a value, 4-NP is fully deprotonated and changed to anionic form. The anionic form of 4-NP may not be completely fitted to the cavities and also, this form of 4-NP is highly water soluble that results in reducing the adsorption affinity of the template on the MIP. On the other hand, at strong acidic conditions, amino functional groups of MIP might be protonated and their effective interactions with 4-NP may also be decreased. This is reasonable because pH has extraordinary influences on the structure of 4-NP and the surface polymer. Therefore, pH 5.0 was selected as optimum pH value for the subsequent experiments.

3.2.2. Effect of adsorption time

The kinetic of adsorption is one of the important factors in defining the adsorption efficiency. The effect of the adsorption time was investigated by varying the shaking time (30–180 min). The kinetic adsorption curve (Fig. 4b) indicated that 90 min was sufficient to achieve the adsorption equilibrium for MMIP even at the concentration of 5 mmol L^{-1}. 4-NP easily reached the surface imprinting cavities of the MIP in the present procedure, and the time it took to reach the adsorption equilibrium was short compared with the time required for that in the traditionally imprinted materials [30,31]. It can be attributed to the nanosized, effective surface imprinting and uniform structures of MIP that exhibited efficient mass transfer and short equilibrium time.

3.2.3. Effect of desorption solvent

The adsorption of 4-NP on the surface of MIP can be carried out by hydrogen bonding interaction between amino-functional group and the template molecules. Using acetic acid, as an eluent, allows disruption of the hydrogen bonding without having any major impact on the polymer morphology and therefore, caused the release of 4-NP into the desorption solvent. In this study, two elution solvents namely acetonitrile containing 10% v/v acetic acid (solvent A) and methanol containing 10% v/v acetic acid (solvent B) were evaluated to desorb the analyte efficiently. The recovery amount of solvent B (97.4%) was higher than that of solvent A (76.3%). Therefore, methanol containing 10% v/v acetic acid was used in all the subsequent experiments.

3.3. Adsorption isotherms

An important factor for the MIP nanoparticles is the adsorption capacity that determines the required amount of sorbent for quantitative removal of the analyte from the solution. To obtain the adsorption capacities of MMIP and MNIP, the adsorption experiments were carried out at different initial concentrations of 4-NP, ranging from 0.1 to 9 mmol L^{-1}. The MMIP and MNIP nanoparticles were exposed to the various concentrations of 4-NP, and the suspensions were stirred at room temperature. After separation with a magnet, the supernatants were analyzed by RP-HPLC. As shown in Fig. 5, the MMIP nanoparticles revealed greatly higher adsorption capacity for 4-NP than that for MNIP. The maximum adsorption capacity of MMIP was almost two-folds as compared to that of MNIP. The results demonstrate that the recognition sites

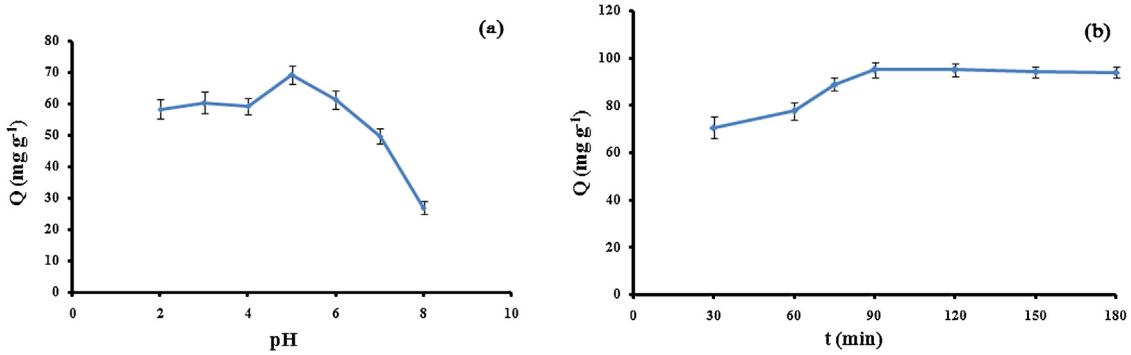

Fig. 4. Adsorption capacity of MMIP at different pH containing the 3 mmol L^{-1} 4-NP in a buffer ranging from 2 to 8 (a), kinetic adsorption curves for 4-NP containing the 5 mmol L^{-1} 4-NP (b).

Table 1
The comparison of "Pre-grafting" MMIP procedure with "Grafting to" MMIP procedure for 4-NP as template.

Type of synthesis	Q_{max} (mg g^{-1})	t^a (min)	$N_{k_{min}-k_{max}}{}^b$	LOQ^c (μg L^{-1})	LOD^d (μg L^{-1})
"Grafting to" 4NP-MMIP	57.8	150	23.42	25	7.24
"Pre-grafting" 4-NP-MMIP	129.1	90	81.80	10	3.6

[a] Time of adsorption.
[b] Number of sites.
[c] Limit of quantitation.
[d] Limit of detection.

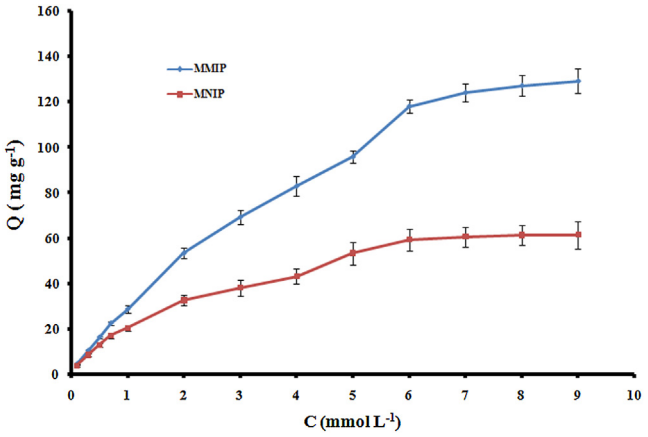

Fig. 5. Adsorption equilibrium isotherm of MMIP and MNIP for 4-NP.

and the amounts of 4-NP bounded to the surface of MMIP were clearly more than those of MNIP. The resulting MIP in this work showed higher Q_{max} than the other corresponding works. In this regard, Tang et al. [35] prepared the MMIP in water media via o-phenylenediamine as a functional monomer. The Q_{max} of 4-NP was obtained 4.5 mg g^{-1} which was lower than that obtained in the present work (129.1 mg g^{-1}). On the other hand, a comprehensive comparison was made between the newly proposed MMIP and our previous MMIP [31]. The obtained results are shown in Table 1. The priority of the pre-grafting procedure was due to the formation of imprinting sites via the template immobilized approach. Therefore, the proposed method can be more efficient than the "Grafting to" method that has so far been a common method for the synthesis MMIP.

For fitting the experimental data, the Langmuir and Freundlich models have been widely used to describe the data by linear regression. When the adsorption is monolayer and indicates homogeneous distribution of energy over the entire coverage surface, the Langmuir isotherm was used, while Freundlich isotherm model is suitable for the multilayer adsorption and heterogeneous binding sites in the imprinted polymers. The experimental data was fitted with Freundlich isotherm and the resulting parameters are summarized in Table 2.

The Freundlich equation can be demonstrated by the Eqs. (5) and (6), where Q_e is the amount of the adsorbed analyte and C_e, is the equilibrium concentration of analyte. In addition, α and m represent Freundlich constant and the heterogeneity index (with values from 0 to 1), respectively. Two additional binding parameters, that is, the number of the binding sites ($N_{k_{min}-k_{max}}$) and the apparent average association constant ($\bar{K}_{k_{min}-k_{max}}$), were also calculated using the Eqs. (7) and (8):

$$Q_e = \alpha C_e^m \quad (5)$$

$$\log\ Q_e = \log\ \alpha + m\log\ C_e \quad (6)$$

$$N_{k_{min}-k_{max}} = \alpha(1-m^2)(k_{min}^{-m} - k_{max}^{-m}) \quad (7)$$

$$\bar{K}_{k_{min}-k_{max}} = \left(\frac{m}{m-1}\right)\left(\frac{k_{min}^{1-m} - k_{max}^{1-m}}{k_{min}^{-m} - k_{max}^{-m}}\right) \quad (8)$$

$$k_{min} = \frac{1}{c_{max}},\ k_{max} = \frac{1}{c_{min}}$$

As it can be seen in Table 2, $N_{k_{min}-k_{max}}$ for MMIP was much higher than that for MNIP. This means that the number of binding sites with adequate geometry and good accessibility to the target analyte in MIP-coated magnetic nanoparticles were higher than those in the NIP-coated magnetic nanoparticles. Thus, the imprinting phenomenon was proved for the target analyte.

The Langmuir model was also studied for fitting the experimental data and the R^2 values (R^2 = 0.959 for MMIP and R^2 = 0.961 for MNIP) obtained were less than those of the Freundlich model. In addition, the related constants of Freundlich equation (such as m and α) are more compatible with the obtained experimental data, while they are not obtained for the related constants of the Langmuir equation. The theoretical adsorption capacity of Langmuir (Q_{max} = 66.67 mg g^{-1} and Q_{max} = 40.49 mg g^{-1} for MMIP and MNIP, respectively) is not adjusted to the real value that is obtained from the experimental data. Hence, the results demonstrate the multilayer adsorption and heterogeneous binding sites in the imprinted polymers.

3.4. Selectivity experiment for 4-NP

For imprinted materials, selective adsorption performance is very important and often demonstrated by comparing the binding extent of the template molecule with other similar structural analogs. In order to verify that the MMIP was selective for 4-NP, the solutions of 2,4-DNP, Ph, 2-NP and 4-NP were individually prepared for testing the binding characteristics of the MMIP and MNIP. Fig. 6 shows the adsorption capacities of the MIP and NIP for 2,4-DNP, Ph, 2-NP and 4-NP molecules with the concentration level of 500 mg L^{-1}. The MMIP exhibited remarkably higher adsorption capacity for the template molecule than the MNIP. The distribution

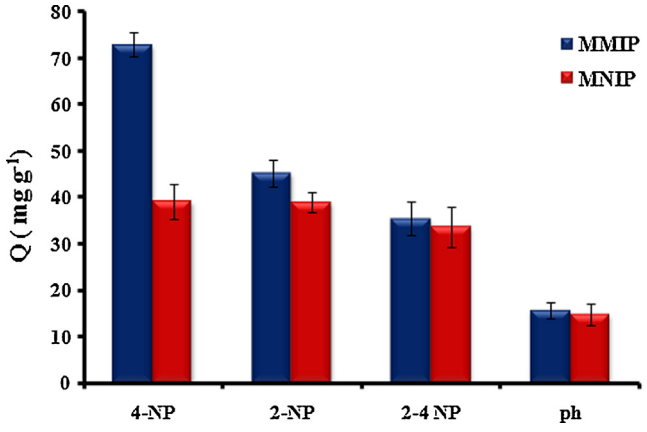

Fig. 6. Adsorption selectivity for 4-NP and analogous compounds by MMIP and MNIP under optimized conditions.

Table 2
Parameters of Freundlich isothermal equation for adsorption experimental data.

Adsorbent	m	α [(mg g^{-1})(L g^{-1}) m]	R^2	$N_{k_{min}-k_{max}}$ (mg g^{-1})	$\bar{K}_{k_{min}-k_{max}}$ (L g^{-1})
4-NP-MMIP	0.664	151.29	0.995	81.80	10.14
4-NP-MNIP	0.539	67.14	0.990	47.80	11.06

Table 3
The selectivity parameters of MMIP and MNIP.

Sample	MMIP		MNIP		
	K_d (mL g^{-1})	α	K_d (mL g^{-1})	α	α_r
4-NP	205.82		92.98		
2-NP	110.65	1.86	92.14	1.01	1.84
2,4-DNP	82.75	2.49	77.90	1.19	2.09
Ph	33.50	6.14	31.46	2.96	2.07

coefficients of 4-NP were higher than that of the similar compounds and the calculated results are listed in Table 3. MMIP exhibited significant adsorption selectivity for 4-NP, compared to the similar structural compounds. It can be attributed to the more suitable binding sites for the template due to an efficient imprinting effect and the difference in the size, functional group's type and position of the analytes, molecular interactions, hydrophobicities and acidic properties of the similar structural compounds.

Phenol has the greatest structural and molecular-interaction difference than 4-NP, among the other compounds, which has resulted in poor selectivity of MMIP for it. The results showed that the selectivity coefficient of 4-NP than those of 2,4-DNP and 2-NP were 2.49 and 1.86, respectively. It illustrated that MMIP was more selective for 2-NP than 2,4-DNP due to the more structural likeness of 2-NP than 2,4-DNP to the template. The imprinting process created cavities that were similar in size and conformational structure to the template. Therefore, the selectivity results were obtained from the imprinting effect owing to the stereochemistry, molecular size recognition and specific interaction of MMIPs toward the template molecules.

3.5. Method validation and real sample analysis

The linear range of the calibration curve for 4-NP was 10–3000 μg L^{-1} with limit of detection (LOD) of 3.6 μg L^{-1}. The LOD value was lower than the allowed limit reported by EPA (<60 μg L^{-1}) in drinking water [22]. Therefore, it indicates that this method can be useful to detect 4-NP in water media according to the guideline level of EPA.

To verify the ability of this method for analysis of real samples, MMIP was used to determine the trace amounts of 4-NP in the seawater in combination with HPLC under optimal conditions. The studied 4-NP was not detected in the seawater. Then, the real

Table 4
Determination of 4-NP in seawater sample by MMIP and MNIP (n = 3).

Sample		MMIP			MNIP		
	Added (μg L^{-1})	Found (μg L^{-1})	Recovery (%)	RSD (%)	Found (μg L^{-1})	Recovery (%)	RSD (%)
Persian Gulf	0	N.D.[a]	–	–	N.D.	–	–
	50	48.01	96.0	2.7	17.32	34.6	7.5
	100	98.51	98.5	2.4	35.64	35.6	3.7

[a] N.D., not detected.

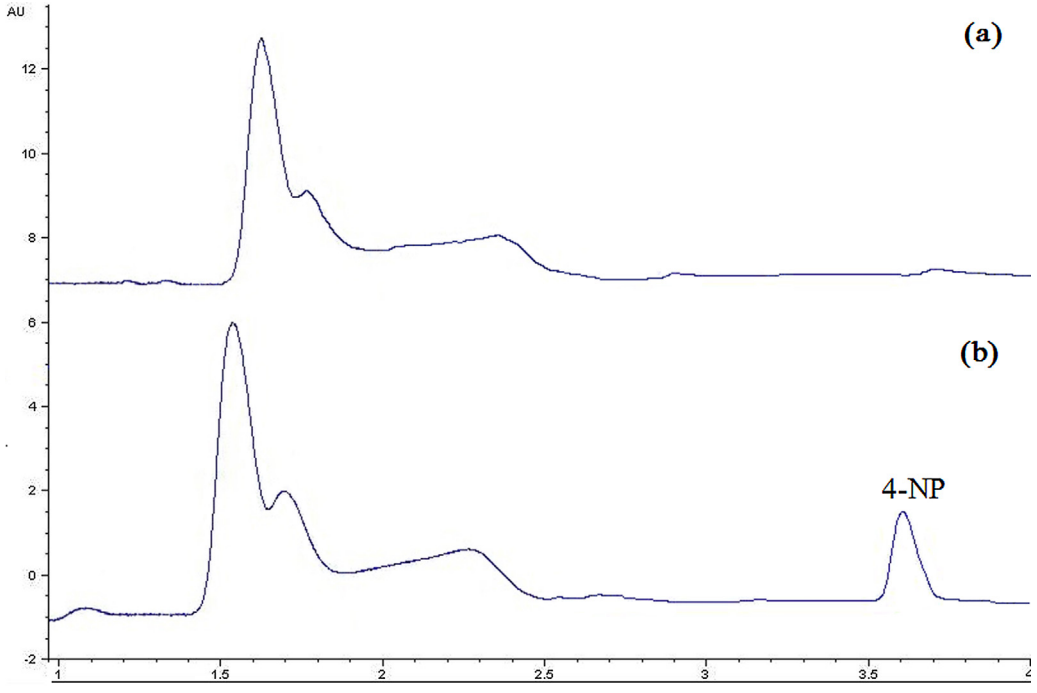

Fig. 7. The chromatograms of extracted 4-NP from Persian Gulf (a) and spiked sample with 100 μg L^{-1} of 4-NP (b) by MMIP.

sample was spiked with 4-NP at two concentration levels of 50 and 100 μg L^{-1}. All the results for the seawater sample extracted by the MMIP and MNIP are collected in the Table 4. When 100 μg L^{-1} of 4-NP was spiked in the real sample, the average recoveries of 4-NP reached 98.5% and 35.6% (n = 3) by using the MMIP and MNIP, respectively. In addition, Fig. 7 illustrates chromatograms of the none-spiked and spiked seawater samples with 100 μg L^{-1} of 4-NP.

4. Conclusions

In summary, a novel surface imprinting method was developed for the construction of MMIP by combination of pre-grafted functional material on the surface of magnetic substrate and surface-immobilized template strategy by using 4-NP as template. Compared with the conventional methods, the present technique improved the binding capacity and kinetics by increasing the amount of the formed imprinting sites for the target analytes due to the immobilization of the template on the surface or in the vicinity of the material's surface. The magnetic MIP was easily collected by an external magnetic field without additional centrifugation or filtration. The results showed that MMIP offers the advantages of high adsorption capacity and selectivity as well as better recovery than MNIP. The presented method has a great potential for the monitoring of the 4-NP in environmental water samples at the concentration level of μg L^{-1}.

References

[1] S. Banerjee, B. König, Molecular imprinting of luminescent vesicles, J. Am. Chem. Soc. 135 (2013) 2967–2970.
[2] Y. Peng, Y. Xie, J. Luo, L. Nie, Y. Chen, L. Chen, Sh. Du, Zh. Zhang, Molecularly imprinted polymer layer-coated silica nanoparticles toward dispersive solid-phase extraction of trace sulfonylurea herbicides from soil and crop samples, Anal. Chim. Acta 674 (2010) 190–200.
[3] X. Ding, P.A. Heiden, Recent developments in molecularly imprinted nanoparticles by surface imprinting techniques, Macromol. Mater. Eng. 299 (2014) 268–282.
[4] L. Qin, X. He, W. Zhang, W. Li, Y. Zhang, Surface-modified polystyrene beads as photografting imprinted polymer matrix for chromatographic separation of proteins, J. Chromatogr. A 1216 (2009) 807–814.
[5] X. Wei, X. Li, S.M. Husson, Surface molecular imprinting by atom transfer radical polymerization, Biomacromolecules 6 (2005) 1113–1121.
[6] X. Li, S.M. Husson, Adsorption of dansylated amino acids on molecularly imprinted surfaces: a surface plasmon resonance study, Biosens. Bioelectron. 22 (2006) 336–348.
[7] Y. Li, C. Dong, J. Chu, J. Qi, X. Li, Surface molecular imprinting onto fluorescein-coated magnetic nanoparticles via reversible addition fragmentation chain transfer polymerization: a facile three-in-one system for recognition and separation of endocrine disrupting chemicals, Nanoscale 3 (2011) 280–287.
[8] S. Wang, R. Wang, X. Wu, Y. Wang, C. Xue, J. Wu, J. Hong, J. Liu, X. Zhou, Magnetic molecularly imprinted nanoparticles based on dendritic-grafting modification for determination of estrogens in plasma samples, J. Chromatogr. B 905 (2012) 105–112.
[9] E. Moczko, A. Poma, A. Guerreiro, I. Perez de Vargas Sansalvador, S. Caygill, F. Canfarotta, M.J. Whitcombe, S. Piletsky, Surface-modified multifunctional MIP nanoparticles, Nanoscale 5 (2013) 3733–3741.
[10] H. Chen, D. Yuan, Y. Li, M. Dong, Z. Chai, J. Kong, G. Fu, Silica nanoparticle supported molecularly imprinted polymer layers with varied degrees of crosslinking for lysozyme recognition, Anal. Chim. Acta 779 (2013) 82–89.
[11] D. Gao, Zh. Zhang, M. Wu, Ch. Xie, G. Guan, D. Wang, A surface functional monomer-directing strategy for highly dense imprinting of TNT at surface of silica nanoparticles, J. Am. Chem. Soc. 129 (2007) 7859–7866.
[12] Sh. Wang, Y. Li, M. Ding, X. Wu, J. Xu, R. Wang, T. Wen, W. Huang, P. Zhou, K. Ma, X. Zhou, Sh. Du, Self-assembly molecularly imprinted polymers of 17β-estradiol on the surface of magnetic nanoparticles for selective separation and detection of estrogenic hormones in feeds, J. Chromatogr. B 879 (2011) 2595–2600.
[13] Zh. Xu, L. Ding, Y. Long, L. Xu, L. Wang, Ch. Xu, Preparation and evaluation of superparamagnetic surface molecularly imprinted polymer nanoparticles for selective extraction of bisphenol A in packed food, Anal. Methods 3 (2011) 1737–1744.
[14] J. Matsui, K. Akamatsu, S. Nishiguchi, D. Miyoshi, H. Nawafune, K. Tamaki, N. Sugimoto, Composite of Au nanoparticles and molecularly imprinted polymer as a sensing material, Anal. Chem. 76 (2004) 1310–1315.
[15] X. Shen, L. Zhu, Ch. Huang, H. Tang, Zh. Yu, F. Deng, Inorganic molecular imprinted titanium dioxide photocatalyst: synthesis, characterization and its application for efficient and selective degradation of phthalate esters, J. Mater. Chem. 19 (2009) 4843–4851.
[16] Y. Zhang, J. Zhang, Ch. Dai, X. Zhou, Sh. Liu, Sorption of carbamazepine from water by magnetic molecularly imprinted polymers based on chitosan-Fe3O4, Carbohyd. Polym. 97 (2013) 809–816.
[17] C.I. Lin, A.K. Joseph, C.K. Chang, Y.D. Lee, Synthesis and photoluminescence study of molecularly imprinted polymers appended onto CdSe/ZnS core-shells, Biosens. Bioelectron. 20 (2004) 127–131.
[18] R.C. Stringer, S. Gangopadhyay, S.A. Grant, Detection of nitroaromatic explosives using a fluorescent-labeled imprinted polymer, Anal. Chem. 82 (2010) 4015–4019.
[19] H. Wang, W. Zhou, X. Yin, Zh. Zhuang, H. Yang, X. Wang, Template synthesized molecularly imprinted polymer nanotube membranes for chemical separations, J. Am. Chem. Soc. 128 (2006) 15954–15955.
[20] H. Ebrahimzadeh, E. Moazzen, M.M. Amini, O. Sadeghi, Novel ion imprinted polymer coated multiwalled carbon nanotubes as a high selective sorbent for determination of gold ions in environmental samples, Chem. Eng. J. 215–216 (2013) 315–321.
[21] X. Yang, Zh. Zhang, J. Li, X. Chen, M. Zhang, L. Luo, Sh. Yao, Novel molecularly imprinted polymers with carbon nanotube as matrix for selective solid-phase extraction of emodin from kiwi fruit root, Food Chem. 145 (2014) 687–693.
[22] Y. Zhou, Zh. Qu, Y. Zeng, T. Zhou, G. Shi, A novel composite of graphene quantum dots and molecularly imprinted polymer for fluorescent detection of paranitrophenol, Biosens. Bioelectron. 52 (2014) 317–323.
[23] L. Chen, B. Li, Application of magnetic molecularly imprinted polymers in analytical chemistry, Anal. Methods 4 (2012) 2613–2621.
[24] D. Yin, M. Ulbricht, Protein-selective adsorbers by molecular imprinting via a novel two-step surface grafting method, J. Mater. Chem. B 1 (2013) 3209–3219.
[25] F. An, B. Gao, X. Feng, Adsorption and recognizing ability of molecular imprinted polymer MIP-PEI/SiO_2 towards phenol, J. Hazard. Mater. 157 (2008) 286–292.
[26] R. Gao, X. Mu, Y. Hao, L. Zhang, J. Zhang, Y. Tang, Combination of surface imprinting and immobilized template techniques for preparation of core-shell molecularly imprinted polymers based on directly amino-modified Fe_3O_4 nanoparticles for specific recognition of bovine hemoglobin, J. Mater. Chem. B 2 (2014) 1733–1741.
[27] W. Guan, Ch. Han, X. Wang, X. Zou, J. Pan, P. Huo, Ch. Li, Molecularly imprinted polymer surfaces as solid-phase extraction sorbents for the extraction of 2-nitrophenol and isomers from environmental water, J. Sep. Sci. 35 (2012) 490–497.
[28] W. Guan, J. Pan, X. Wang, W. Hu, L. Xu, X. Zou, Ch. Li, Selective recognition of 4-nitrophenol from aqueous solution by molecularly imprinted polymers with functionalized tetratitanate whisker composites as support, J. Sep. Sci. 34 (2011) 1244–1252.
[29] E. Caro, N. Masqué, R.M. Marcé, F. Borrull, P.A.G. Cormack, D.C. Sherrington, Non-covalent and semi-covalent molecularly imprinted polymers for selective on-line solid-phase extraction of 4-nitrophenol from water samples, J. Chromatogr. A 963 (2002) 169–178.
[30] A. Ersöz, A. Denizli, İ. Şener, A. Atilir, S. Diltemiz, R. Say, Removal of phenolic compounds with nitrophenol-imprinted polymer based on π–π and hydrogen-bonding interactions, Sep. Purif. Technol. 38 (2004) 173–179.
[31] A. Mehdinia, T. Baradaran Kayyal, A. Jabbari, M.O. Aziz-Zanjani, E. Ziaei, Magnetic molecularly imprinted nanoparticles based on grafting polymerization for selective detection of 4-nitrophenol in aqueous samples, J. Chromatogr. A 1283 (2013) 82–88.
[32] M. Zarejousheghani, M. Möder, H. Borsdorf, A new strategy for synthesis of an in-tube molecularly imprinted polymer-solid phase microextraction device: selective off-line extraction of 4-nitrophenol as an example of priority pollutants from environmental water samples, Anal. Chim. Acta 798 (2013) 48–55.
[33] R. Lucena, B.M. Simonet, S. Cárdenas, M. Valcárcel, Potential of nanoparticles in sample preparation, J. Chromatogr. A 1218 (2011) 620–637.
[34] B.D. Mather, K. Viswanathan, K.M. Miller, T.E. Long, Michael addition reactions in macromolecular design for emerging technologies, Prog. Polym. Sci. 31 (2006) 487–531.
[35] H. Tang, L. Zhu, Ch. Yu, X. Shen, Selective photocatalysis mediated by magnetic molecularly imprinted polymers, Sep. Purif. Technol. 95 (2012) 165–171.